HyspIRI Sunglint Subgroup: Glint Characterization, Determination of Impacts on Science, and Potential Mitigation Approaches

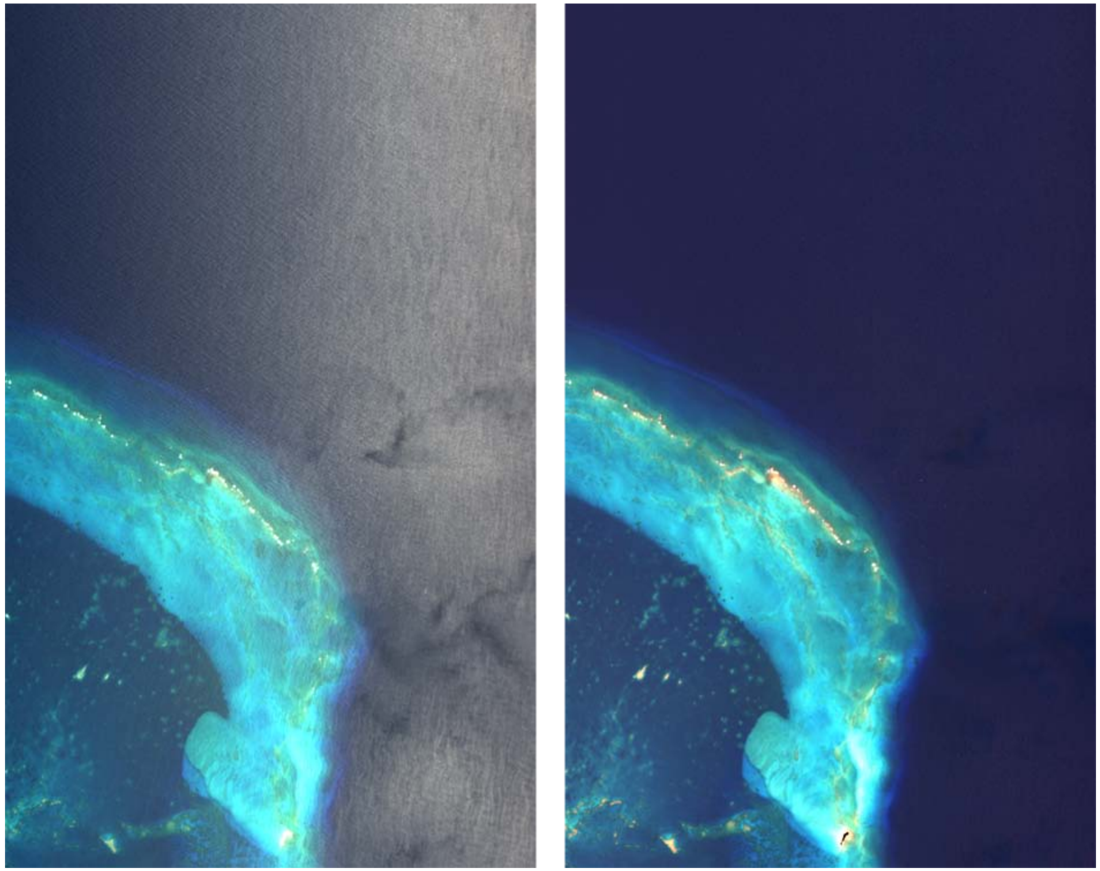

Contributors

Eric J. Hochberg, Curtis D. Mobley, Youngje Park, James Goodman, Kevin R. Turpie, Bo-Cai Gao, Carl F. Bruce, Robert O. Green, Robert G. Knox, Frank E. Muller-Karger, Elizabeth M. Middleton, Peter J. Minnet, Chelle Gentemann, Bogdan V. Oaida, Richard C. Zimmerman

Sources of light contributing to the remotely sensed signal

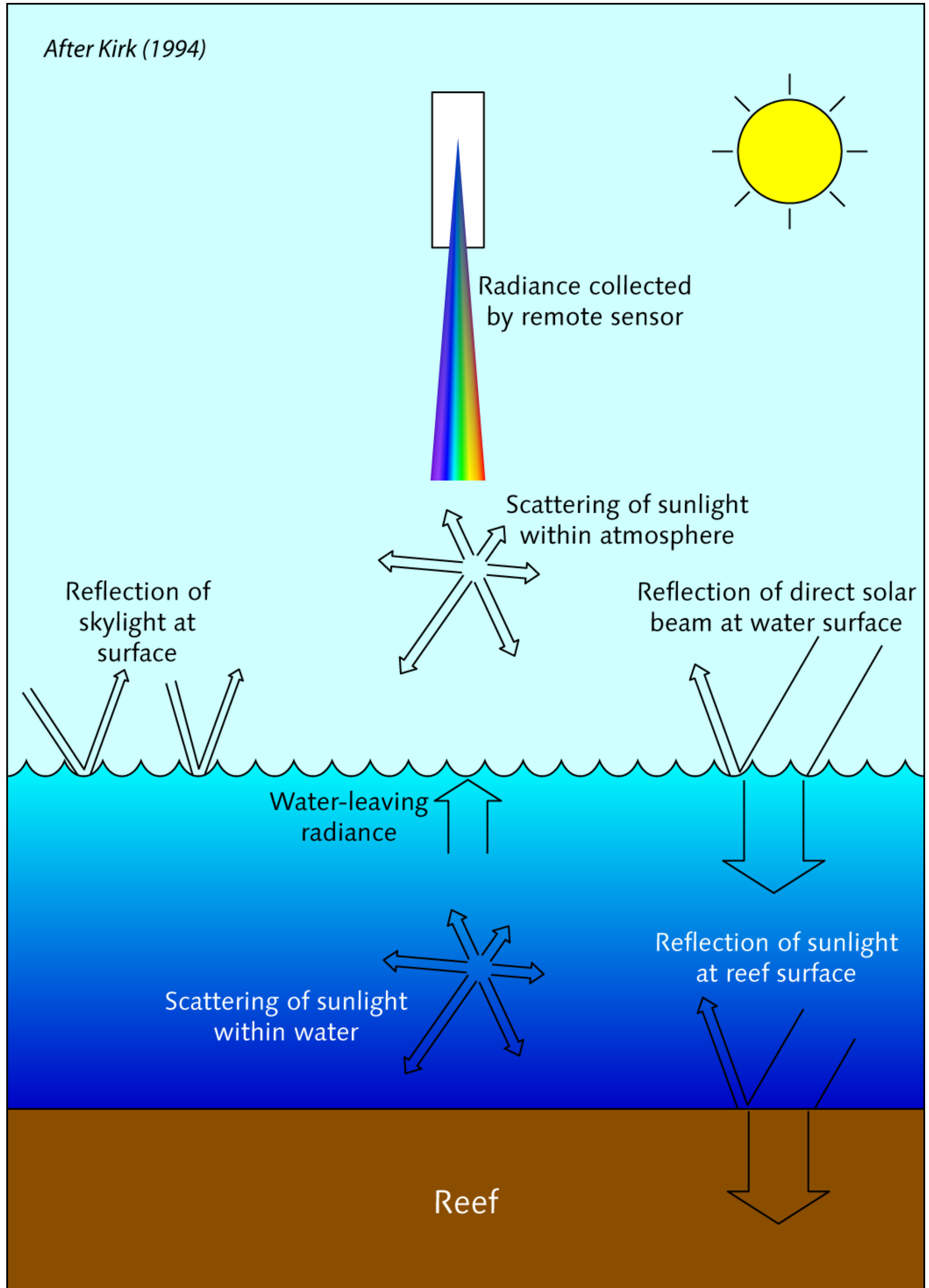

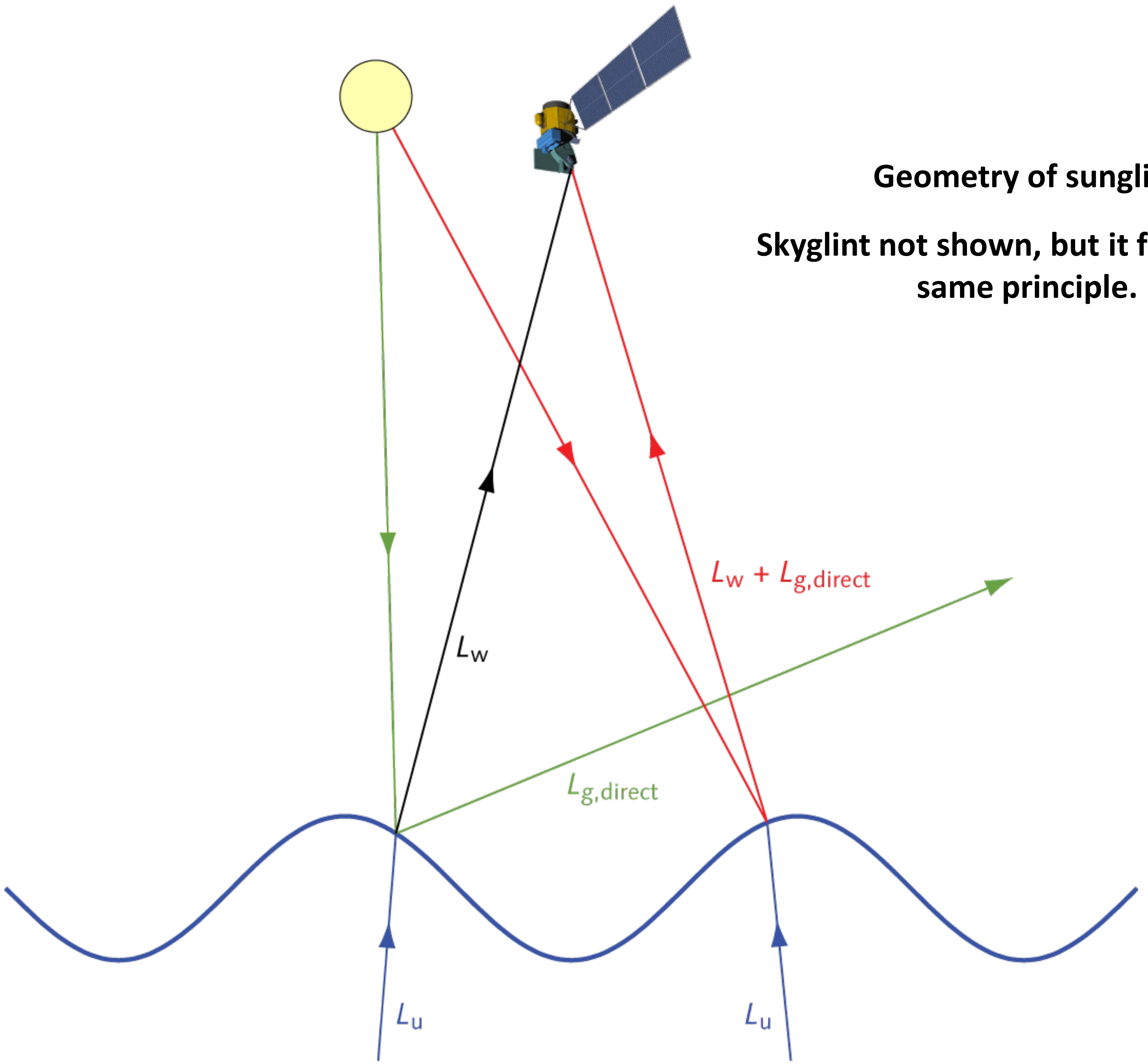

Geometry of sunglint

Skyglint not shown, but it follows the same principle.

Quickbird Example: Tampa Bay, Florida
Very calm water. No apparent sunglint, only skyglint.

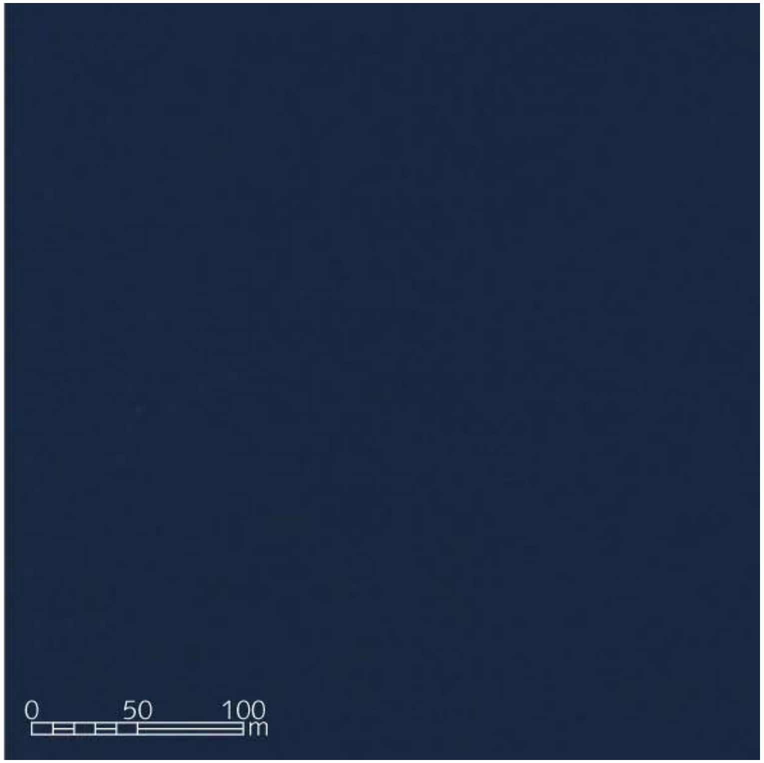

Quickbird Example: Kaneohe Bay, Oahu, Hawaii
Slight wind. Capillary waves engender some sunglint, skyglint implicit.

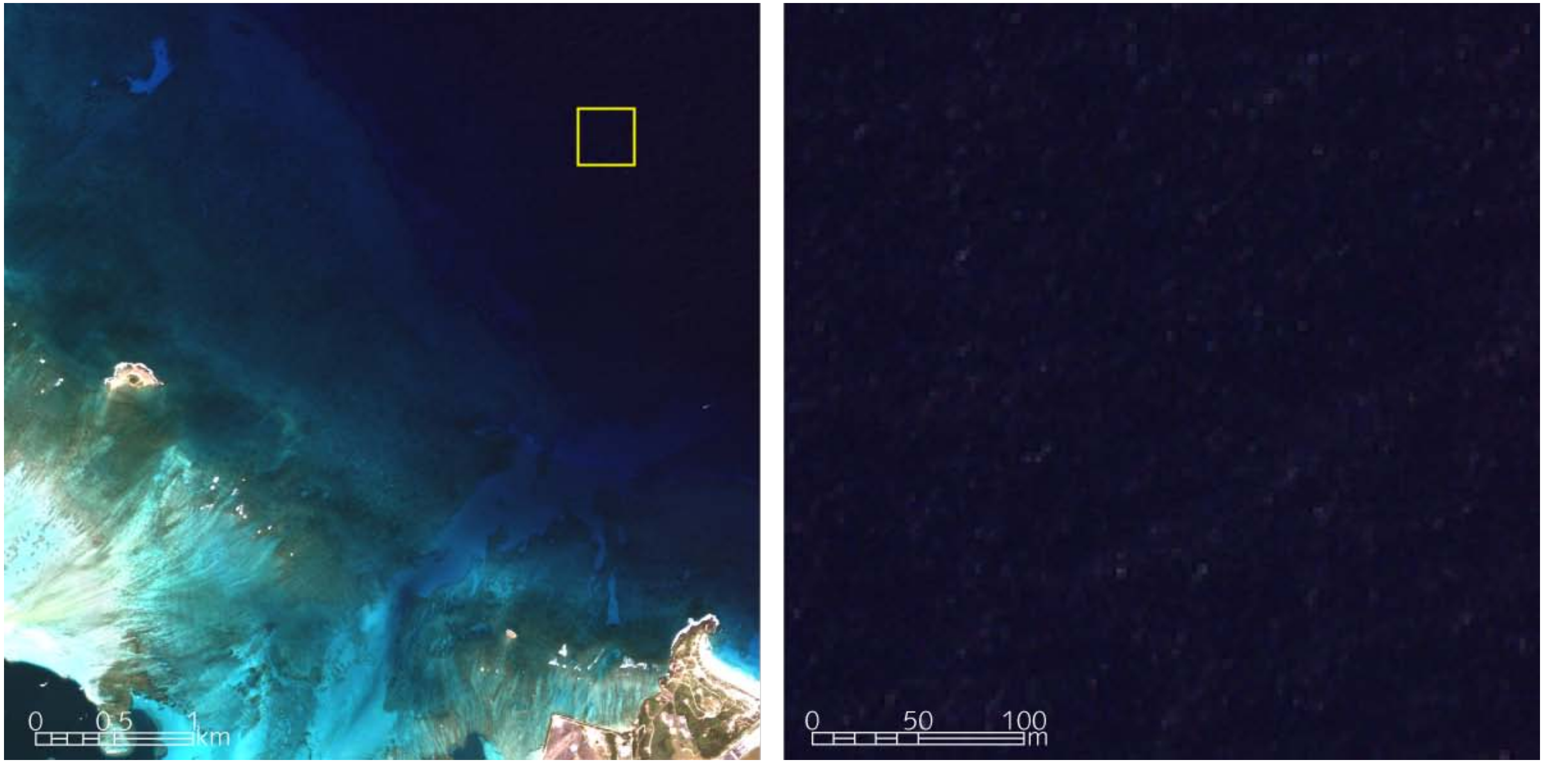

Quickbird Example: Punaluu, Oahu, Hawaii
Trade wind swell. Sunglint on wave faces, skyglint implicit.

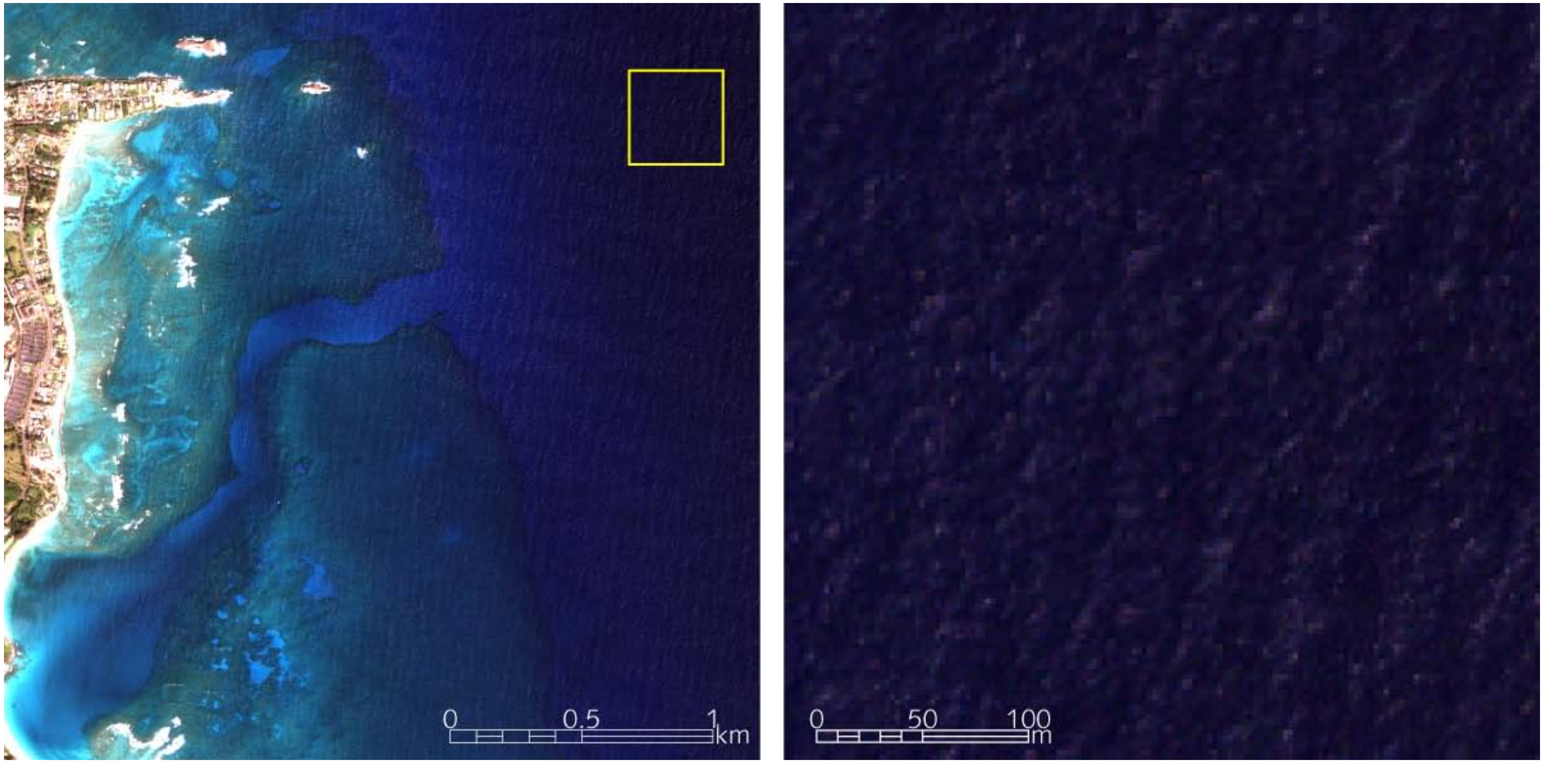

Quickbird Example: Bermuda
Fairly confused sea state. Sunglint on wave faces, skyglint implicit.

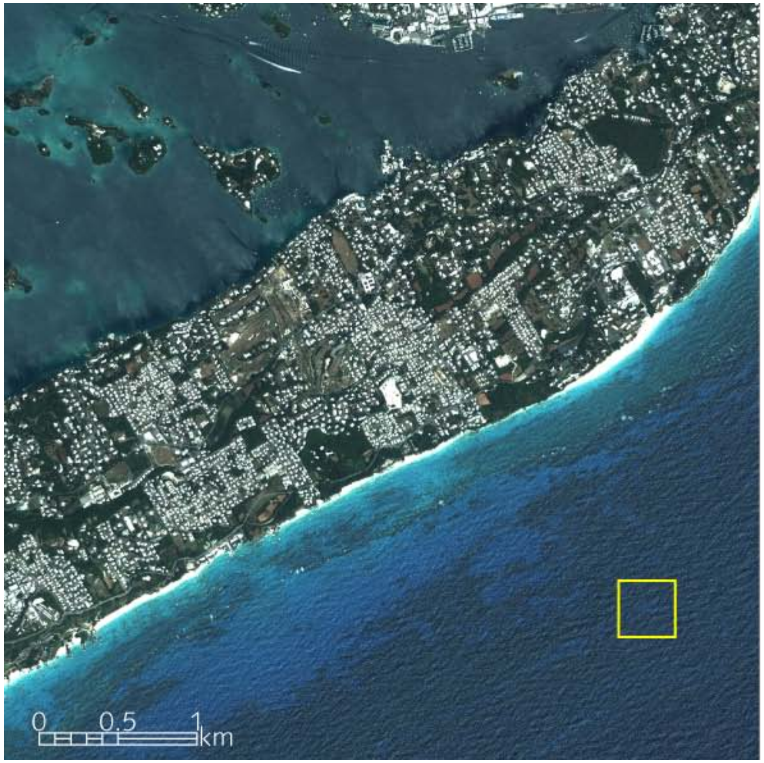

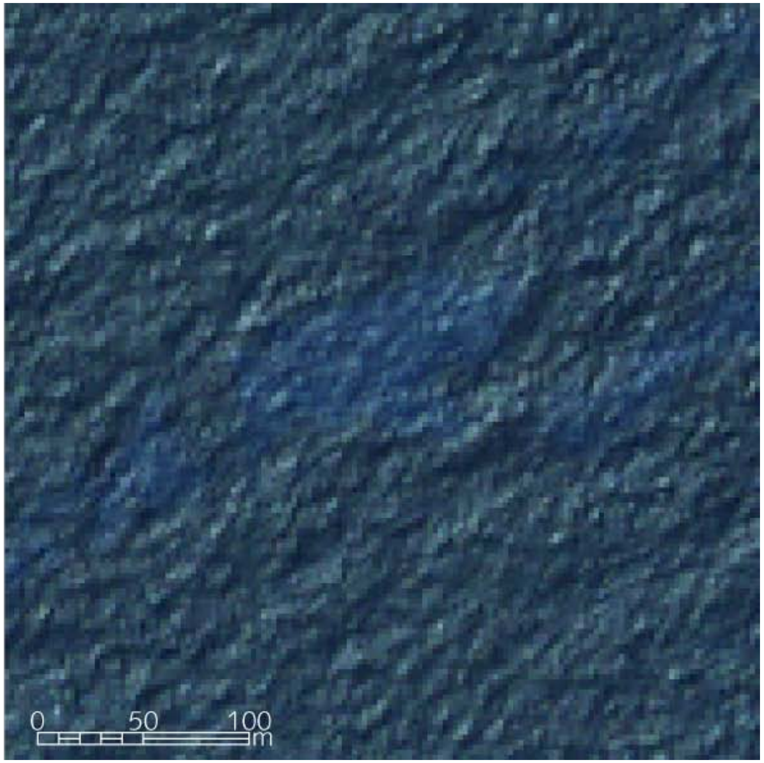

HyspIRI observation geometry. The satellite is moving south (outward from the page).

These view angles, coupled with sun angles, may lead to glint in HyspIRI aquatic scenes.

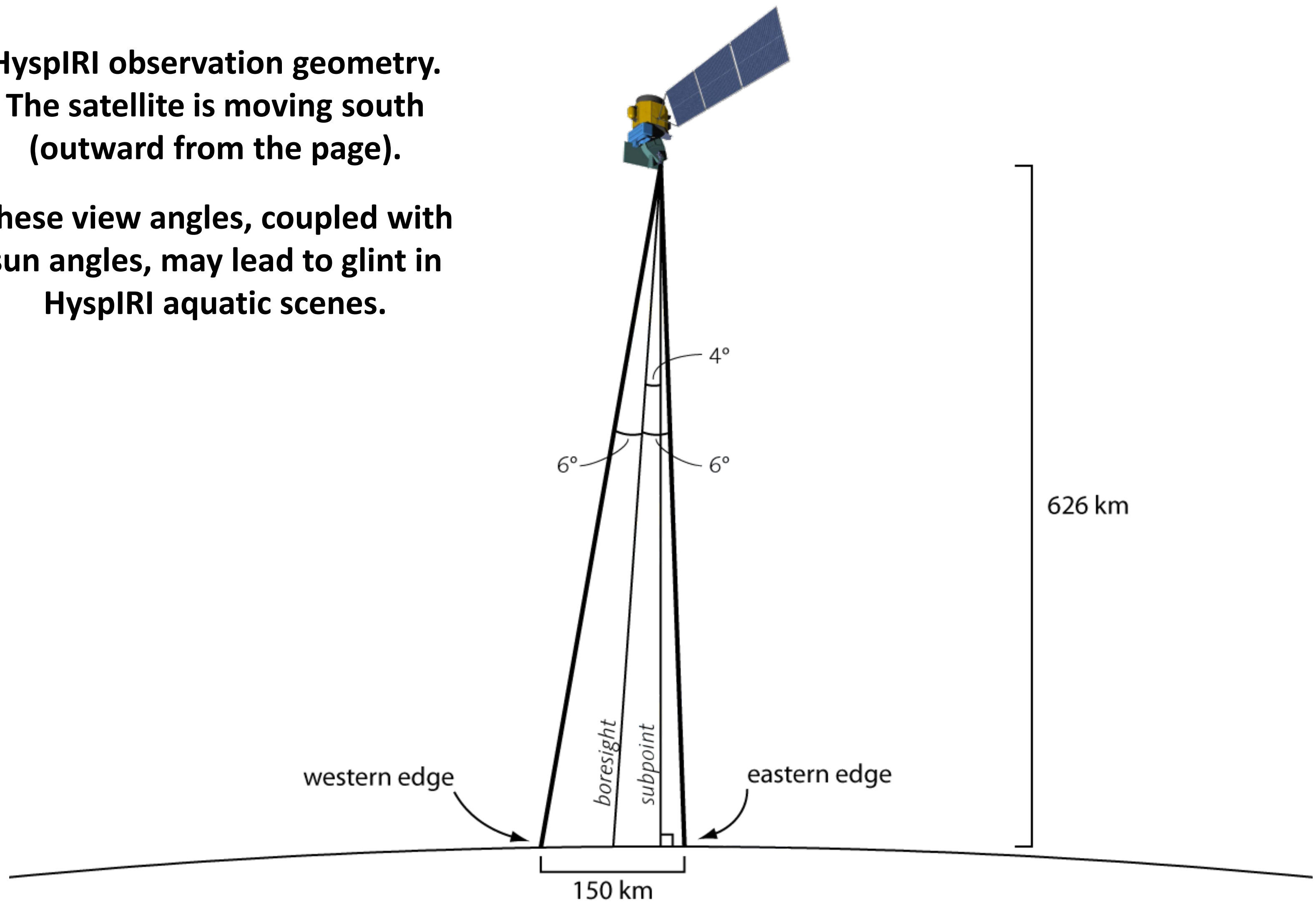

HyspIRI Sunglint Subgroup organization of activities

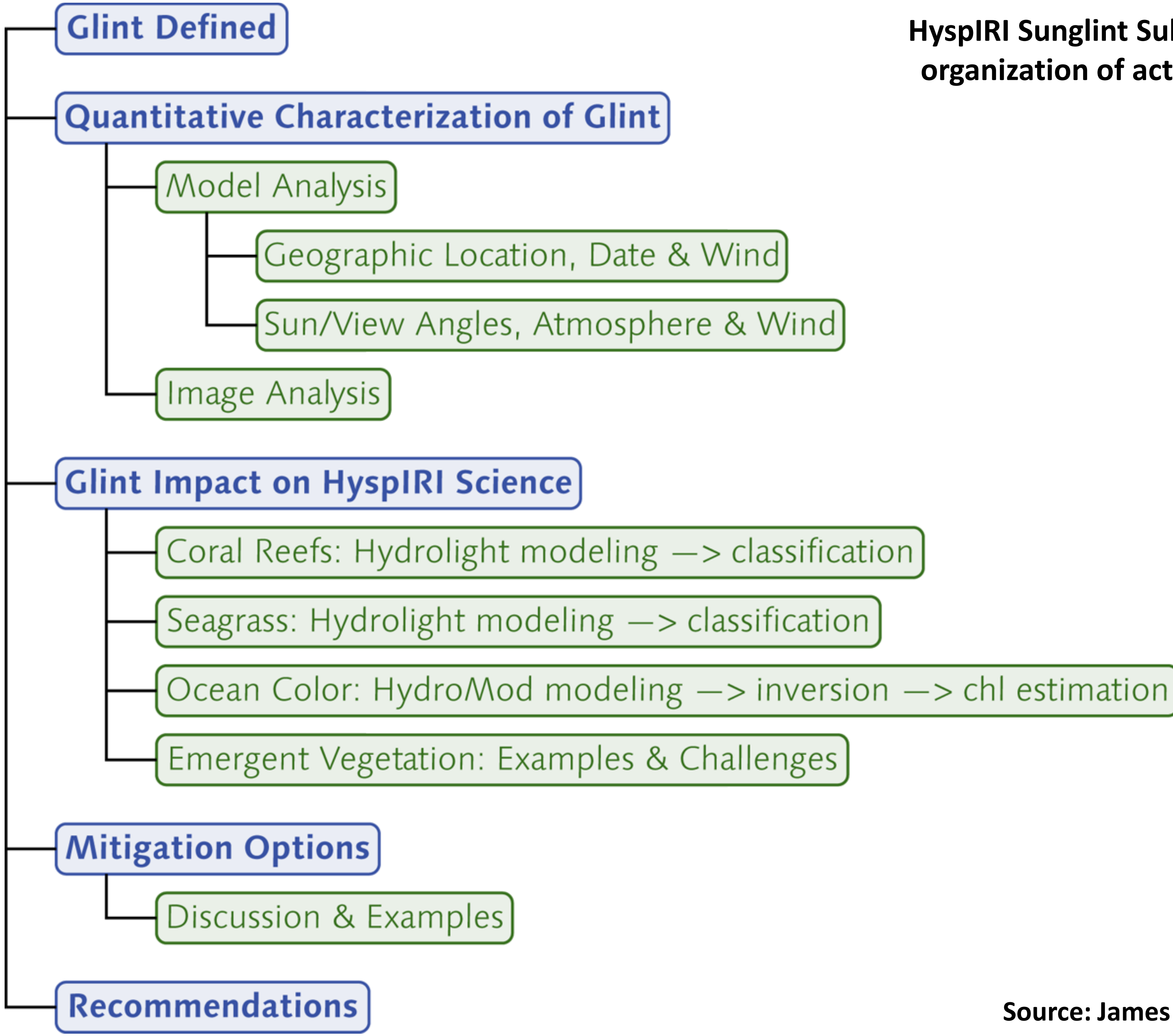

Source: James Goodman

Literature Review

- Glint has been recognized as a potentially confounding factor from the outset of ocean remote sensing.

- There is a fair amount of research on the subject.

- Review of glint and some mitigation strategies:

Kay S, Hedley JD, Lavender S (2009) Sun glint correction of high and low spatial resolution images of aquatic scenes: a review of methods for visible and near-infrared wavelengths. *Remote Sensing* 1:697-730

Approaches to glint mitigation

(A) Avoidance

- Physically pointing the remote sensor toward the ocean at an angle that minimizes specular reflection at the sea surface

- Pointing angle is determined by the position of the sensor relative to the position of the sun, generally assuming the ocean is smooth

(B) Correction

- Even in cases where the bulk of direct specular reflection can be avoided, skyglint contamination remains, as does sunglint that arises due to deviations from the level-surface ocean, i.e., waves

Two basic approaches to glint correction

(1) Statistical modeling of sea surface state to infer glint contribution

- Traced to Cox and Munk (1954), who analyzed aerial photographs of sun glint to infer statistics of the sea surface wave slope distribution as a function of wind speed

- Basis for modern ocean color glint correction

(2) Direct estimation of glint from remote sensing image data

- Based on common assumption that there is no water-leaving radiance in the NIR, especially at l > 900 nm: after atmosphere corrections, remaining NIR signals must originate from the sea surface, i.e., glint

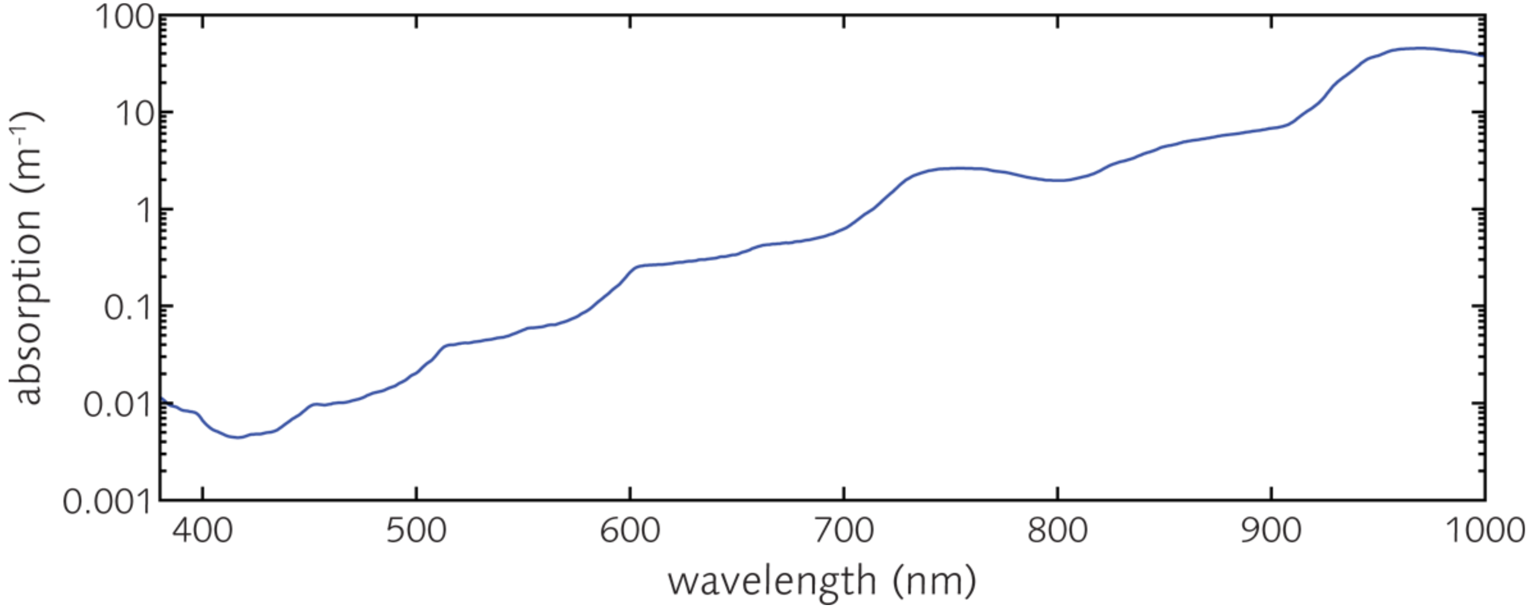

Water absorbs light very strongly at NIR wavelengths, especially >900 nm. Water-leaving radiance at these wavelengths is negligible. VIS data from Pope and Fry (1997); NIR data from Kou et al. (1993).

Direct estimation of glint from remote sensing image data

- There is a linear relationship between glint radiances in VIS and NIR.

- Enables interactive, empirical approaches to glint correction (e.g., Tassan 1994; Hochberg et al. 2003; Hedley et al. 2005; Lyzenga et al. 2006)

- The linear relationship between VIS and NIR glint radiances has a physical basis: the index of refraction of seawater is (nearly) the same at VIS and NIR wavelengths.

- Thus, the reflectance of the water surface is (nearly) spectrally flat, i.e., glint has the same reflectance at VIS and NIR wavelengths.

- The basis for an empirical correction that does not require human interaction (Gao et al. 2000): after atmospheric correction, any remaining NIR reflectance is due to glint. This glint reflectance can simply be subtracted from VIS wavelengths, leaving only water-leaving reflectance.

Literature Review

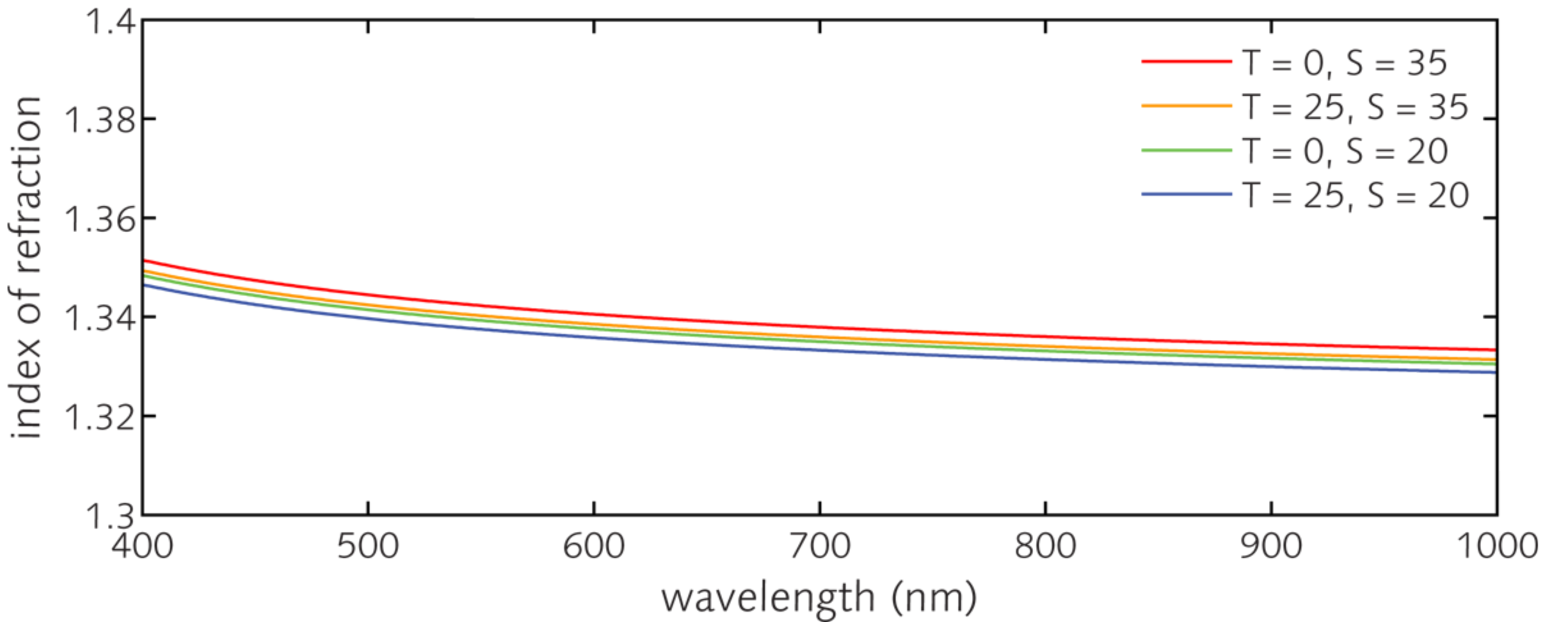

Index of refraction of water. Values are calculated following empirical model of Quan and Fry (1995). Values are modeled for four combinations of temperature (T, ° C) and salinity (S, ‰).

Quantitative Characterization of Glint:
Modeling Based on Latitude, Date, and Wind

Global longitudinal variability of sea-surface sun glint reflectance for the HyspIRI orbit for (a) three levels of wind speed, which were used to compute sea-surface glint at (b) the west edge, (c) the middle point, and (d) the east edge of the HyspIRI field of view.

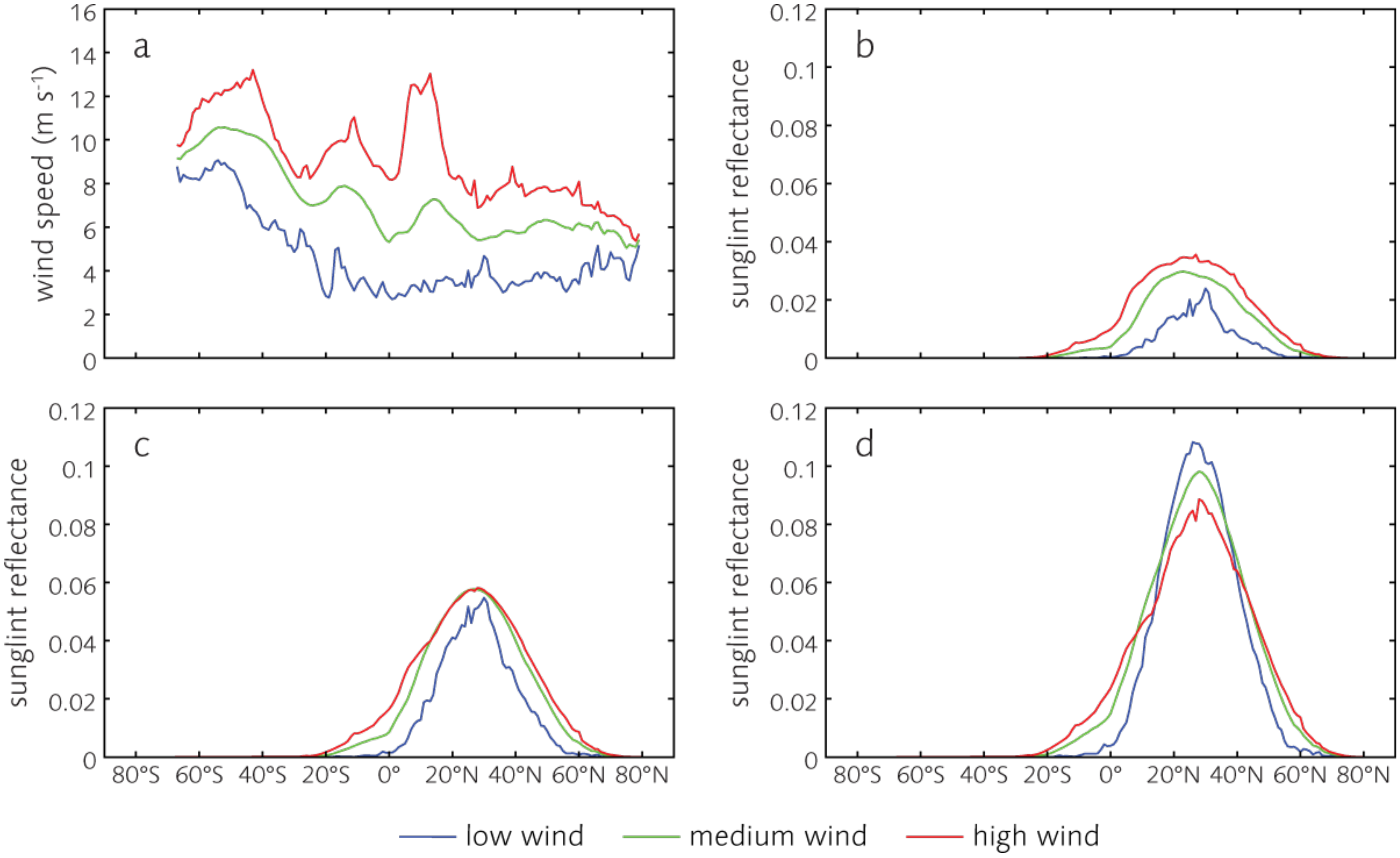

21 June

Source: Youngje Park

Quantitative Characterization of Glint: Modeling Based on Latitude, Date, and Wind

Sea-surface sun glint reflectance variability in a 15° longitudal band (165°W–150°W) for the HyspIRI orbit at (a) three levels of wind speed, which were used to compute sea-surface glint at (b) the west edge, (c) the middle point, and (d) the east edge of the HyspIRI field of view.

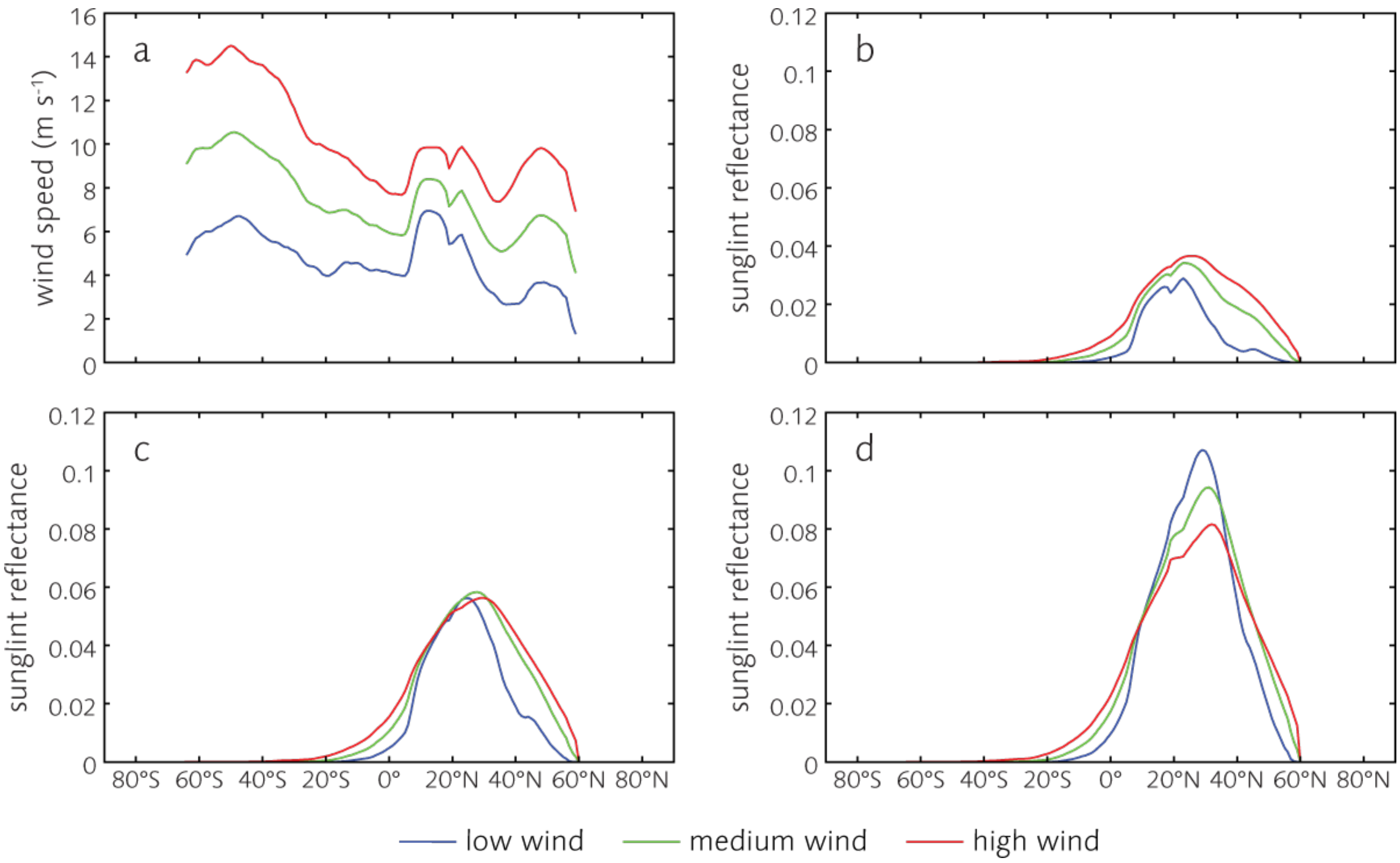

21 June

Source: Youngje Park

Glint Impact on HyspIRI Science:
Modeling Based on Sun/View Angles, Atmosphere and Wind

Example Hydrolight/HydroMod discretized output. Radiance travels outward from center of hemispheres.

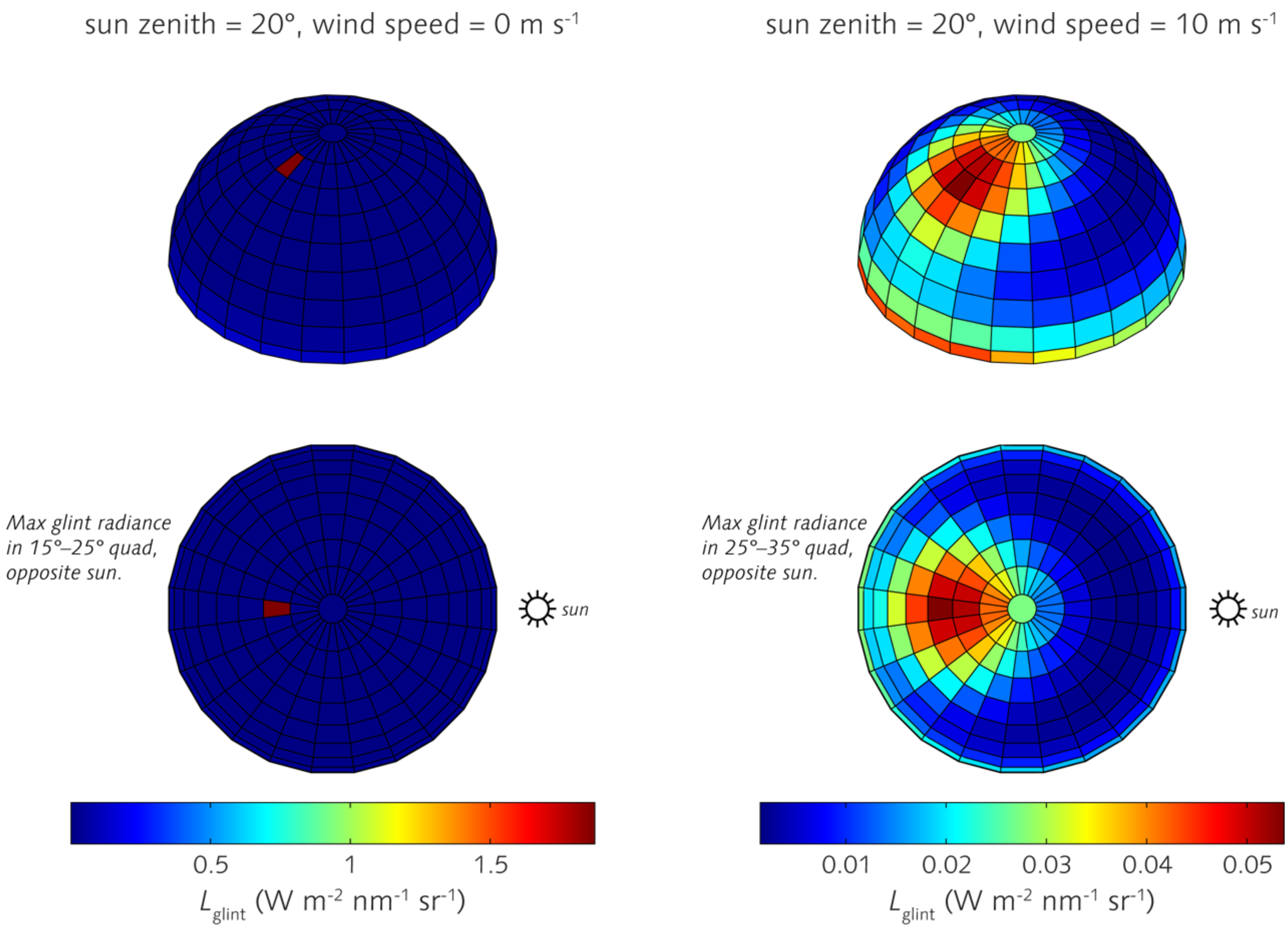

Note difference in radiance scales.

Quantitative Characterization of Glint:
Modeling Based on Sun/View Angles, Atmosphere and Wind

HydroMod simulation of shallow water, mixed bottom spectrum, case 1 inherent optical properties, and comparing east vs. west side of HyspIRI field of view

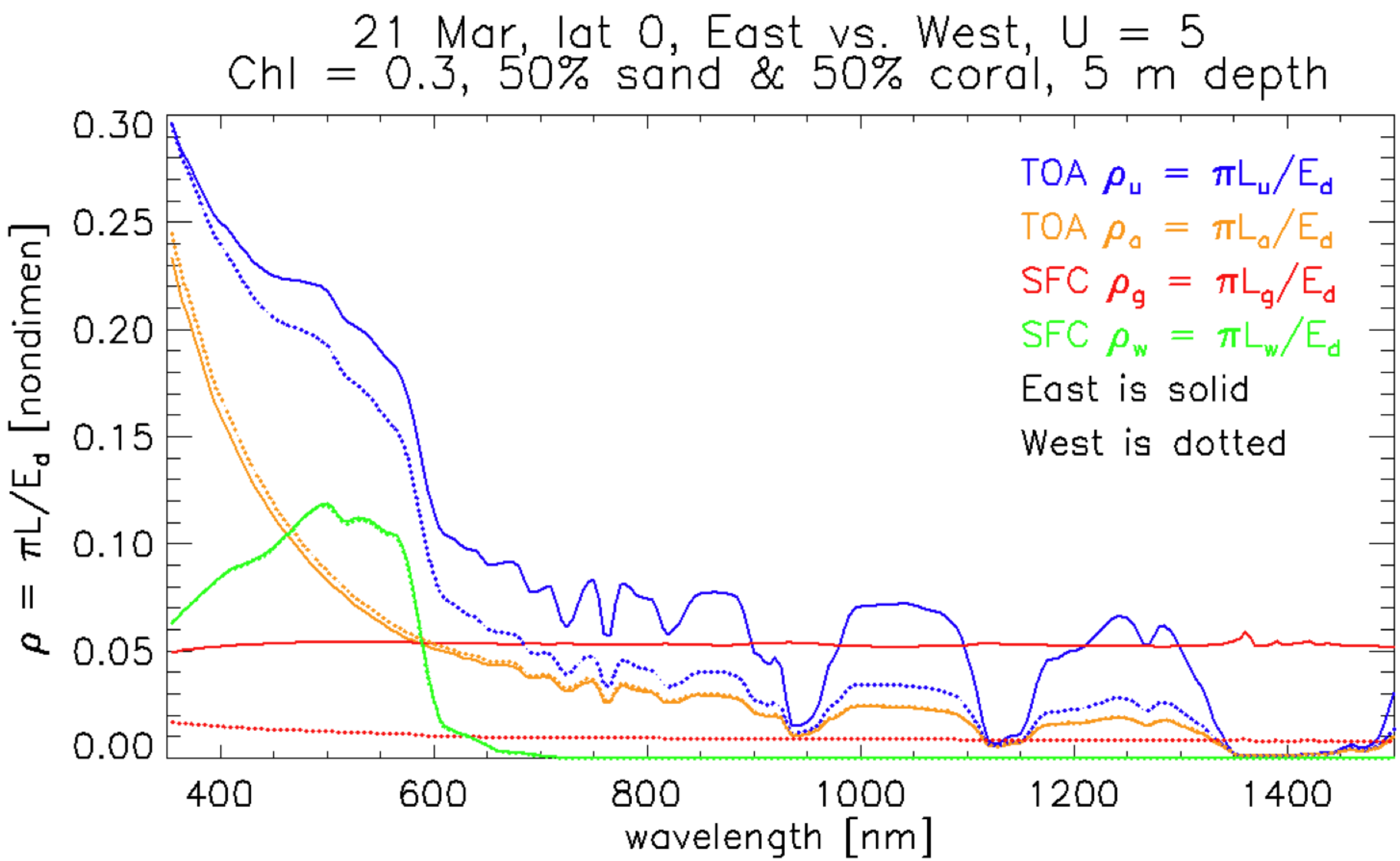

Source: Curtis Mobley

Quantitative Characterization of Glint:
Modeling Based on Sun/View Angles, Atmosphere and Wind

HydroMod simulation of east side of HyspIRI field of view, comparison between shallow water with low chlorophyll and deep water with high chlorophyll

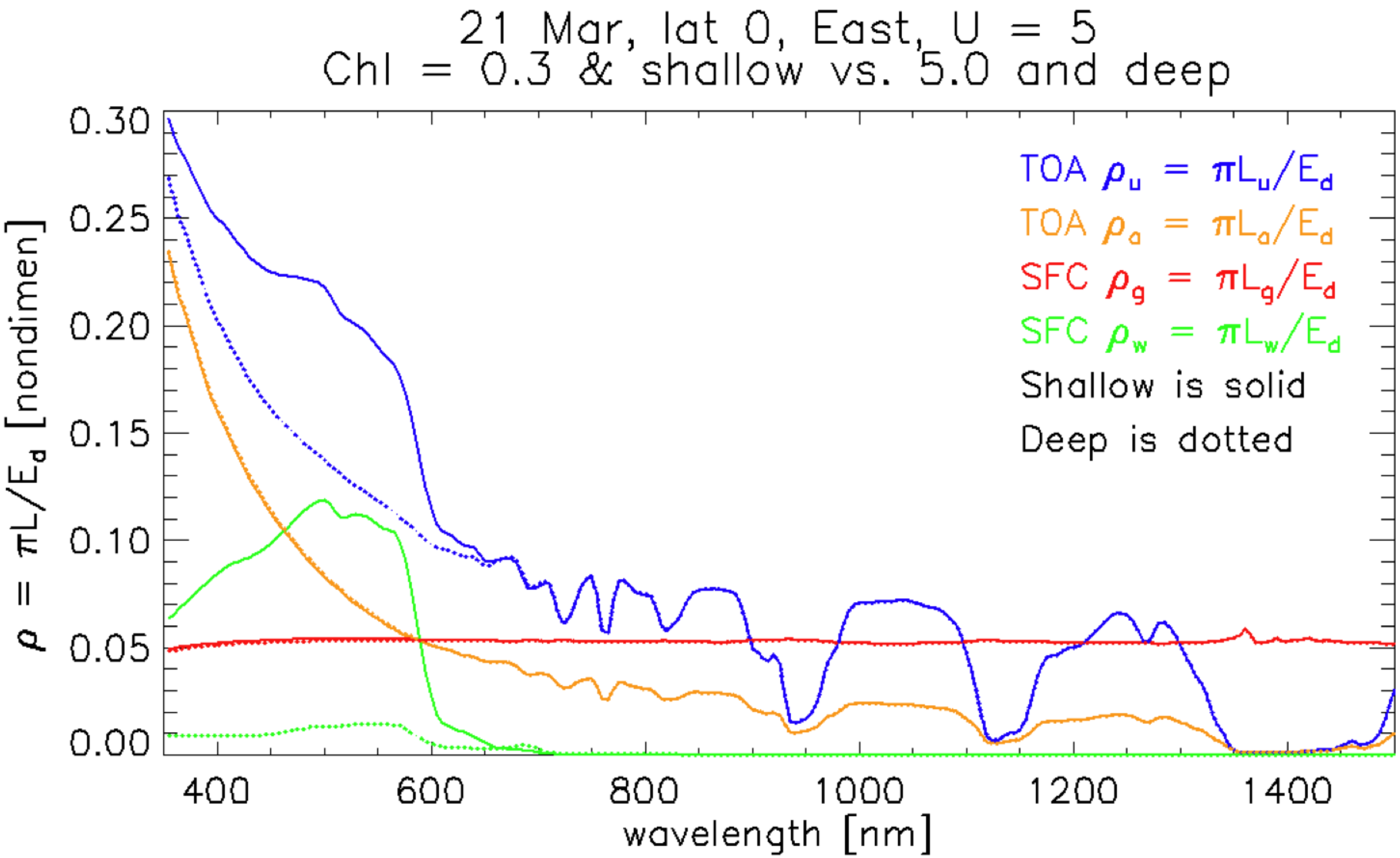

Source: Curtis Mobley

Quantitative Characterization of Glint:
Deriving Glint Statistics from AVIRIS Imagery

AVIRIS scenes used to estimate glint reflectance for comparison with modeled values. Yellow regions are deep-water areas used to extract glint statistics.

f000411t01p03_r01

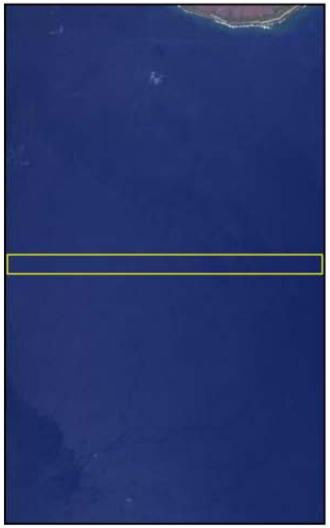

f000412t01p03_r08

f000416t01p03_r02

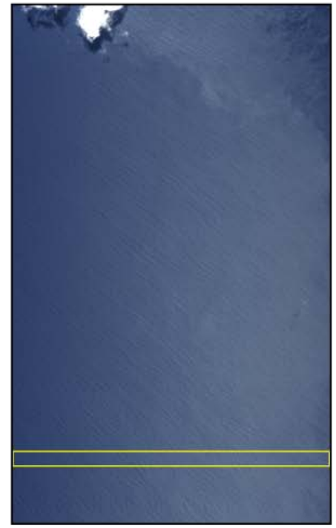

f000416t01p03_r03

f000418t01p03_r01

f000424t01p03_r09

f000425t01p03_r07

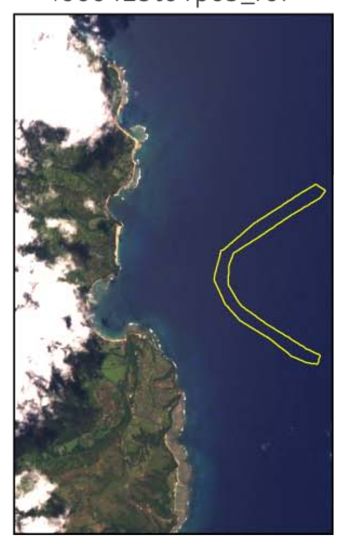

Quantitative Characterization of Glint:
Deriving Glint Statistics from AVIRIS Imagery

Estimated TOA maximum glint reflectances for seven AVIRIS scenes. These values are comparable to modeled values.

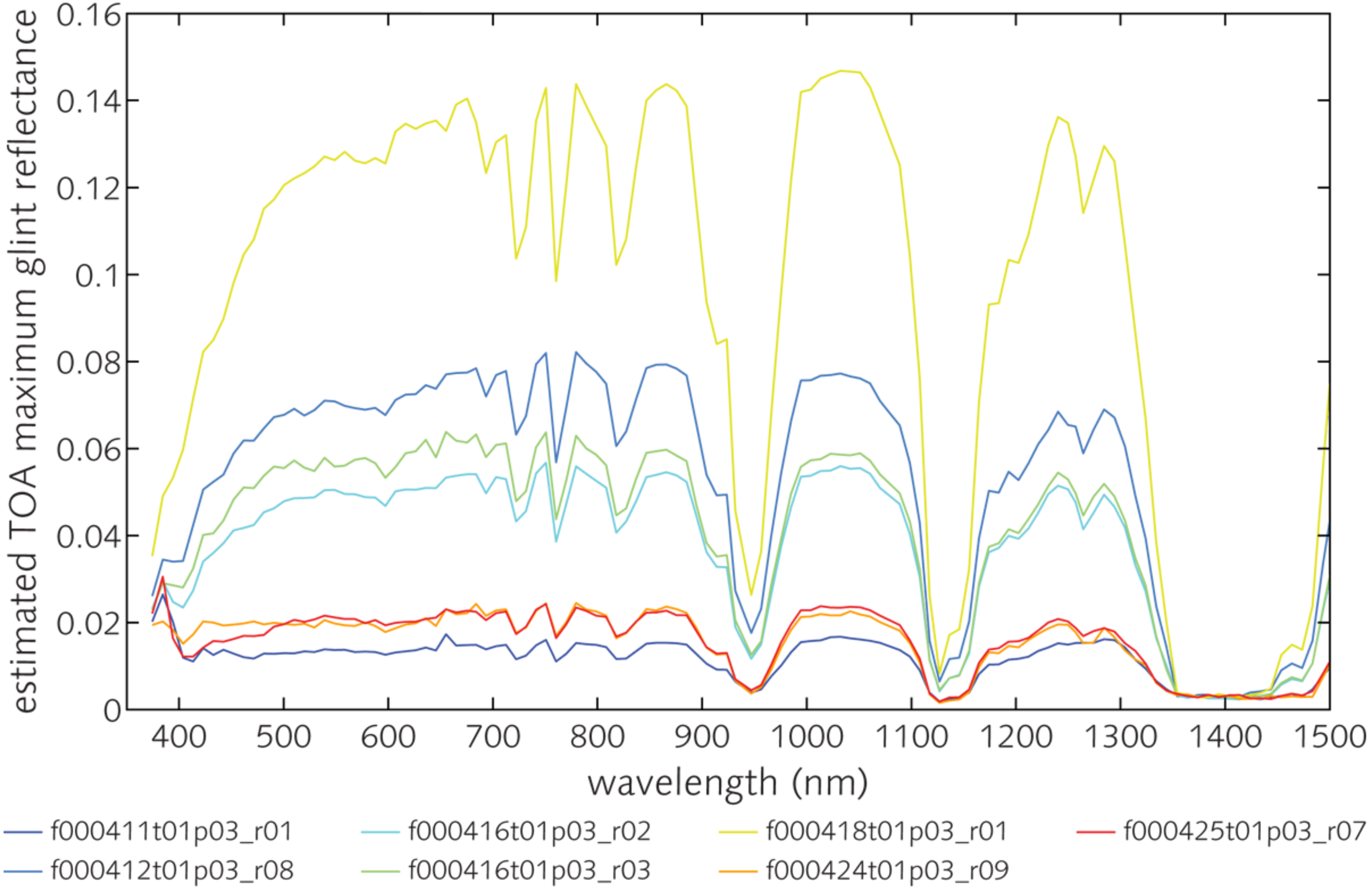

Quantitative Characterization of Glint:
Deriving Glint Statistics from AVIRIS Imagery

AVIRIS scene f000418t01p03_r01 for demonstration of glint-aerosol discimination
Yellow line shows location of cross-track sample in analysis

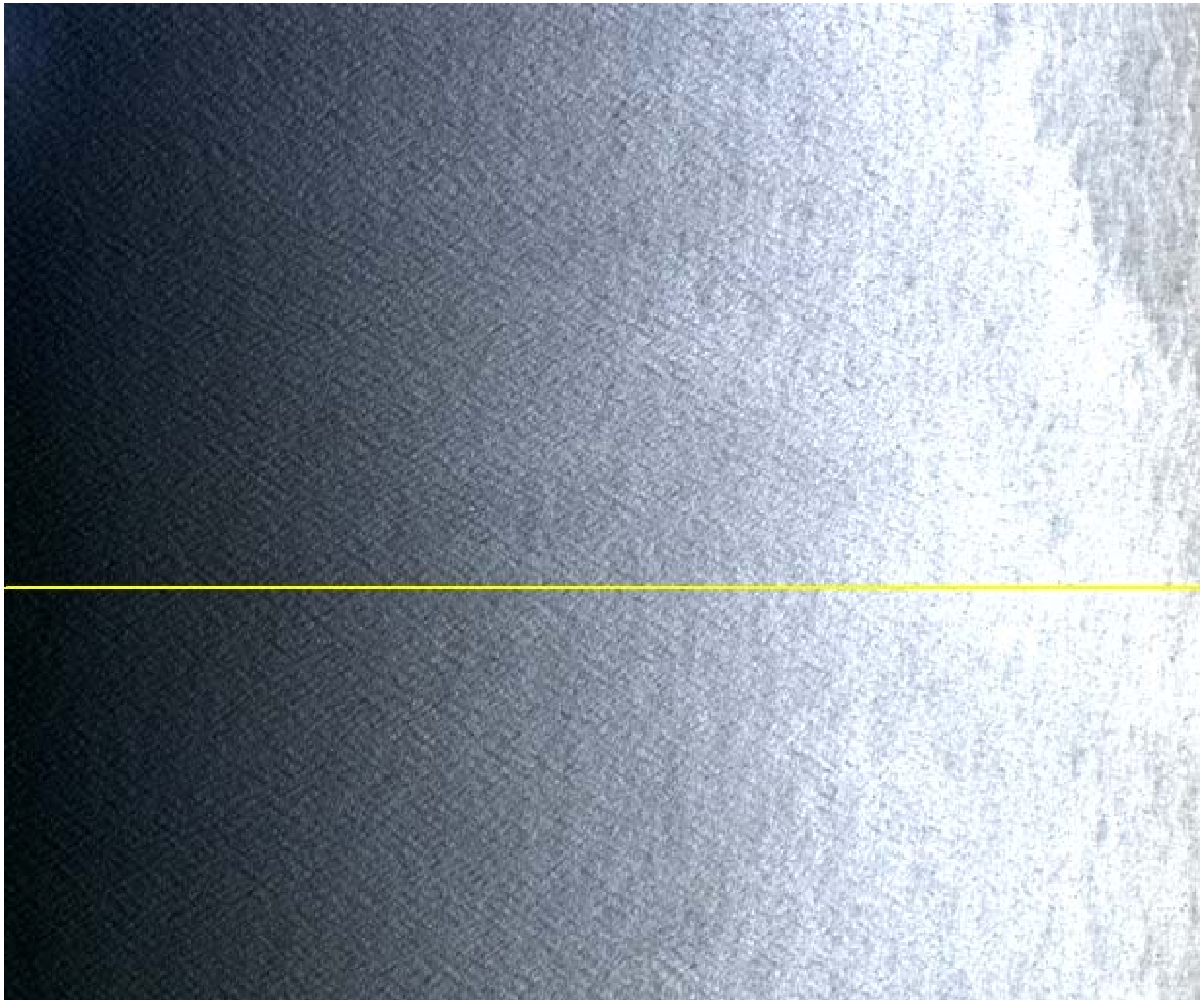

Source: Youngje Park

Quantitative Characterization of Glint: Deriving Glint Statistics from AVIRIS Imagery

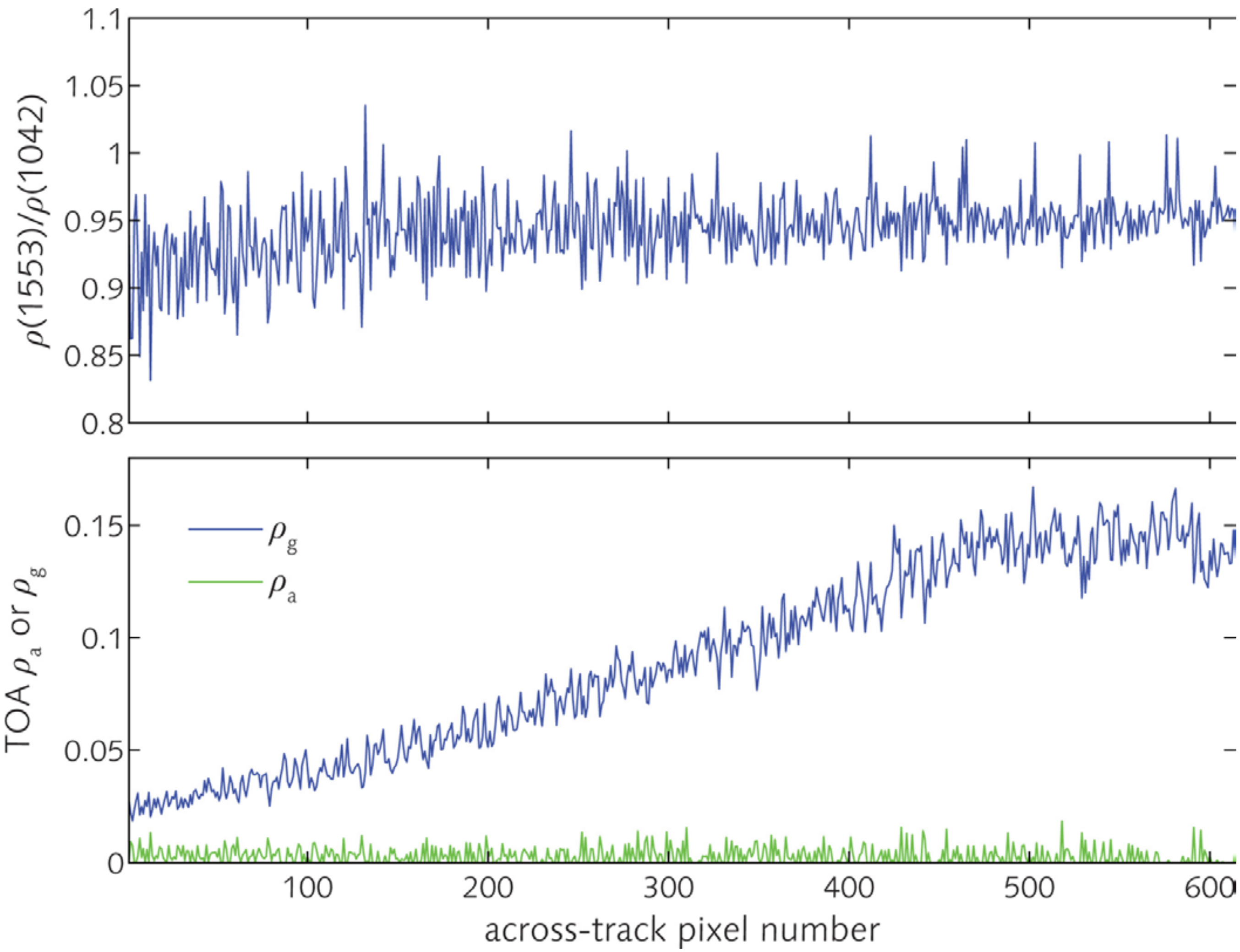

Source: Youngje Park

Quantitative Characterization of Glint: Summary

Several summary observations can be made from model and image analysis:

- The effect of latitude is very clear. Sun glint is stronger where the sun is high, because HyspIRI looks almost straight down. Sun glint effects are apparent across a latitude band of 50° to 100° (i.e., 25° S–25° N to 50° S–50° N), depending on wind speed and the across-track pixel location.
- Sun glint is sensitive to wind speed for low to moderate glint strength and less sensitive for high glint.
- Sun glint at the east edge of the HyspIRI field of view is consistently stronger (a factor of two) than at the west edge.
- Sun glint is high in summer due to high sun and low in winter due to low sun. At the equator in the middle point of the swath, sun glint reflectance takes values of 0.025, 0.01, 0.04 to 0.01 for March, June, September and December respectively.
- Regional temporal variability appears similar to global longitudinal variability in magnitude.
- Large differences in glint reflectance than can occur from the east to the west edges of the HyspIRI field of view for moderate wind speeds in equatorial regions.
- Glint intensity can surpass that of water-leaving radiance.
- Glint radiance is function of incident irradiance.
- Glint reflectance is a function of the index of refraction of the water body.
- *Glint reflectance at the sea surface, to first order, is spectrally flat.* This is particularly important, because it is the basis for virtually all glint correction strategies.

Glint Impact on HyspIRI Science:
Coral Reefs: Hydrolight Modeling & Classification

Scenario 1: Clear reef water, sun zenith 20°, wind 5 m s^{-1}

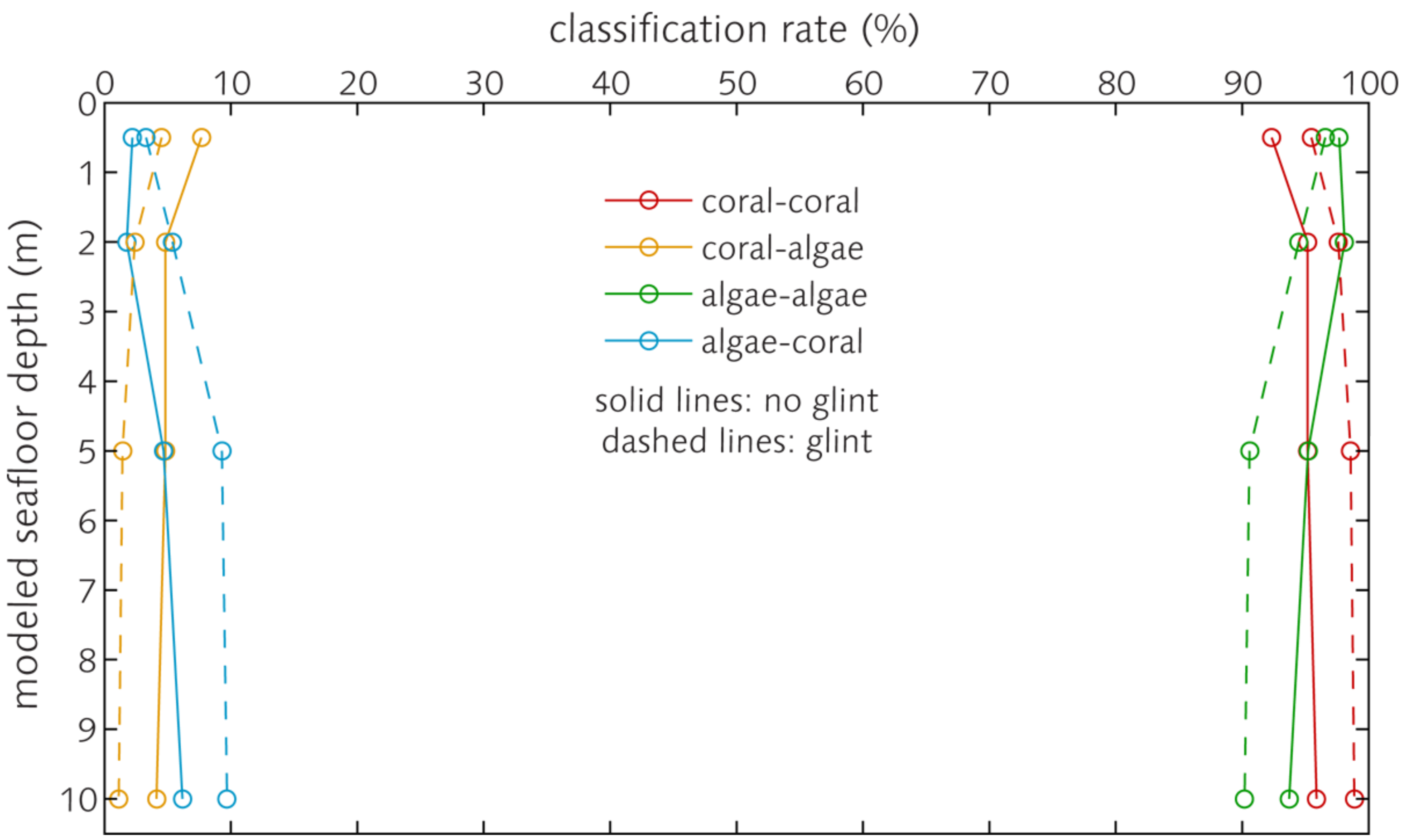

Values indicate classification rates for specific bottom-type/depth combinations classified as bottom-type at any depth. Solid lines show results of R_{rs} modeled without glint; dashed lines show results of R_{rs} modeled with full glint. Under the given water column and view conditions, glint actually increases the correct classification rate of coral at all depths, but it also increases the misclassification of algae as coral at all depths.

Glint Impact on HyspIRI Science:
Coral Reefs: Hydrolight Modeling & Classification

Scenario 2: Turbid reef water, sun zenith 40° , wind 10 m s^{-1}

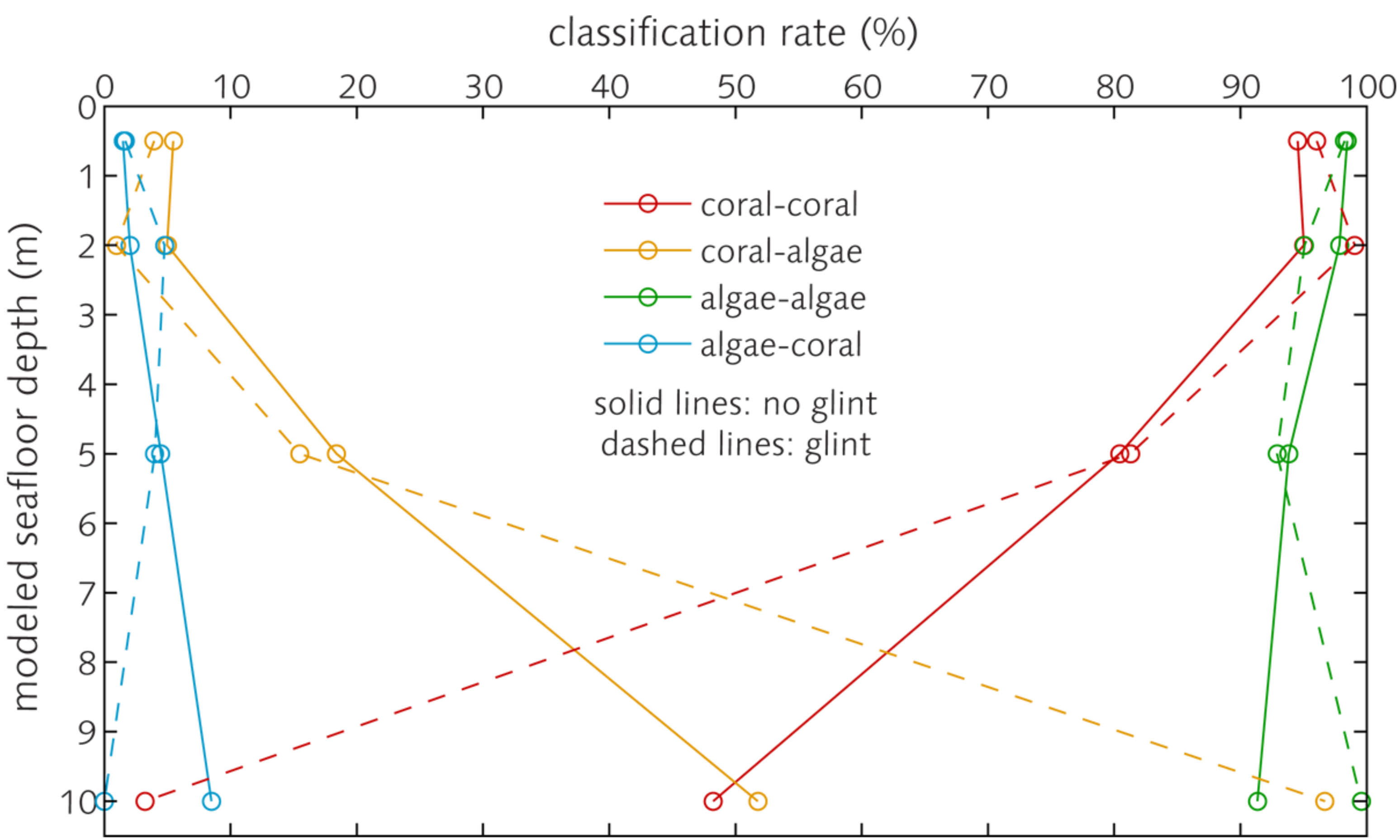

Under these conditions, glint increases the correct classification rate of coral at 0.5 and 2 m, but but greatly reduces correct coral classifications at 10 m.

Glint Impact on HyspIRI Science:
Ocean Color: HydroMod Modeling, Inversion & Analysis

HydroMod parameterization

Location:	Station ALOHA, 22° 45'N, 158° W
Date:	21 June
Sun Azimuth wrt Along Track:	107.78°
Sun Zeinth:	17.99°
Suspended Chlorophyll:	0.05 µg l^{-1}
Wind Speed:	two values modeled, 0 and 10 m s^{-1}
Atmosphere Conditions:	Clear sky with marine aerosols
Bottom Boundary:	Infinitely deep ocean

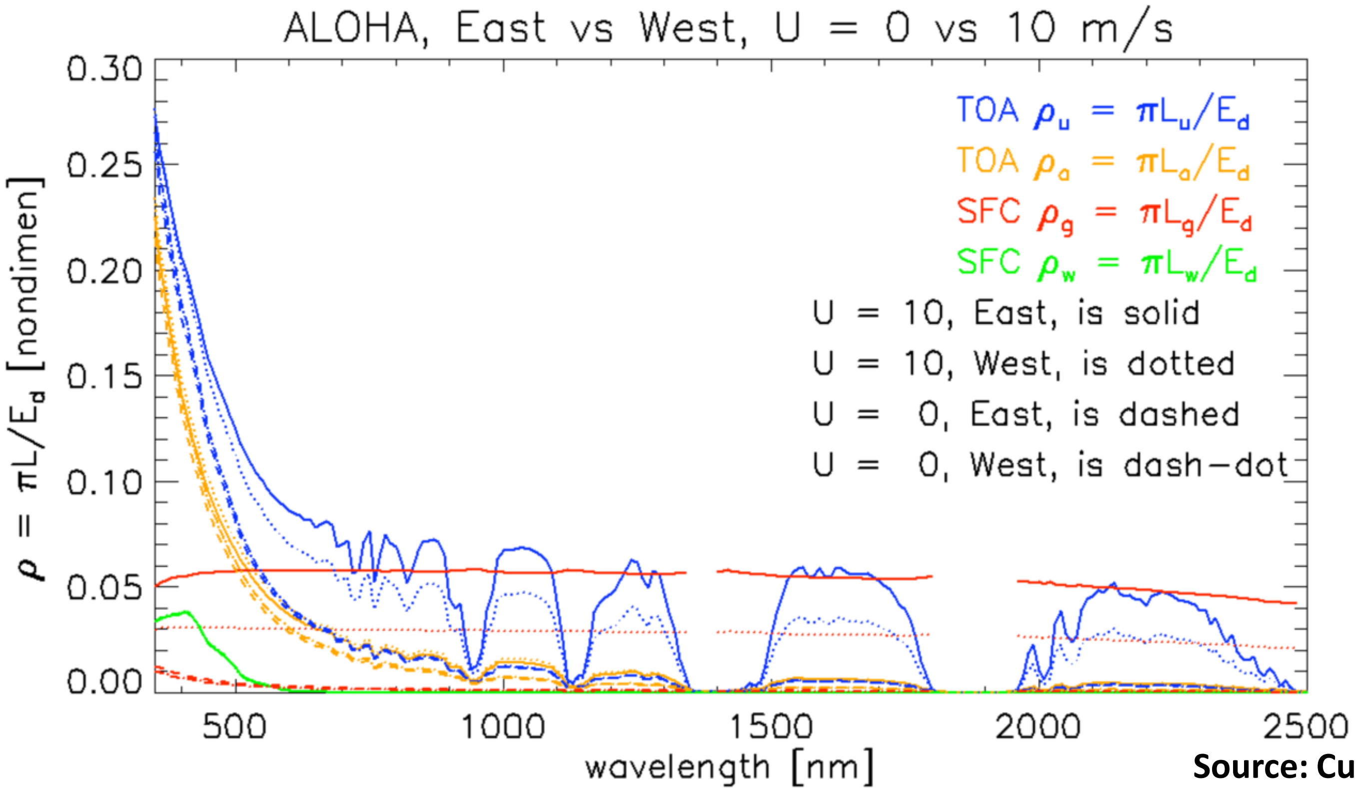

Source: Curtis D. Mobley

Glint Impact on HyspIRI Science:
Ocean Color: HydroMod Modeling, Inversion & Analysis

Radiometrically inverted water-leaving reflectance spectra for Station ALOHA 21 June simulation. (A) West edge of HyspIRI field of view, *U* = 0 m s^{-1}, (B) east edge, *U* = 0 m s^{-1}, (C) west edge, *U* = 10 m s^{-1}, (D) east edge, *U* = 10 m s^{-1}.

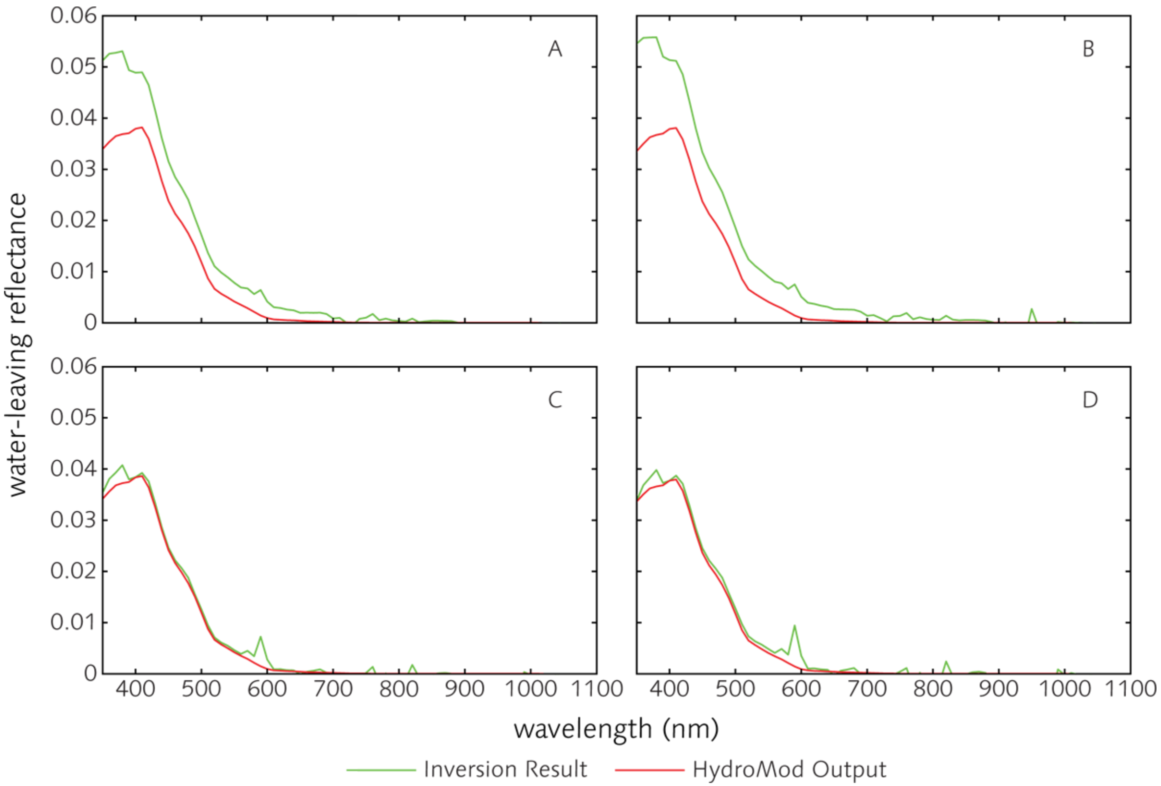

Chlorophyll values (mg m^{-3}) retrieved using OC4 and OC3M algorithms applied to R_{rs} data derived from Figure 4.3.3-2. "Edge" refers to position in HyspIRI field of view. "*U*" refers to wind speed. Actual chlorophyll concentration used in HydroMod biooptical model is 0.05 mg m^{-3}.

Edge	*U* (m s^{-1})	Algorithm	
		OC4	OC3M
West	0	0.12	0.12
East	0	0.14	0.13
West	10	0.08	0.07
East	10	0.08	0.08

Source: Youngje Park

Glint Impact on HyspIRI Science:
Emergent Vegetation: Examples & Challenges

Multi-angle CHRIS/Proba images of Fishing Bay Wildlife Management Area, Maryland. (a) At 0° nominal view zenith angle glint is visually apparent on water bodies interspersed amongst subaerial vegetation. (b) At 55° nominal view zenith angle glint is much less apparent. Boxes cover same ground area in (a) and (b).

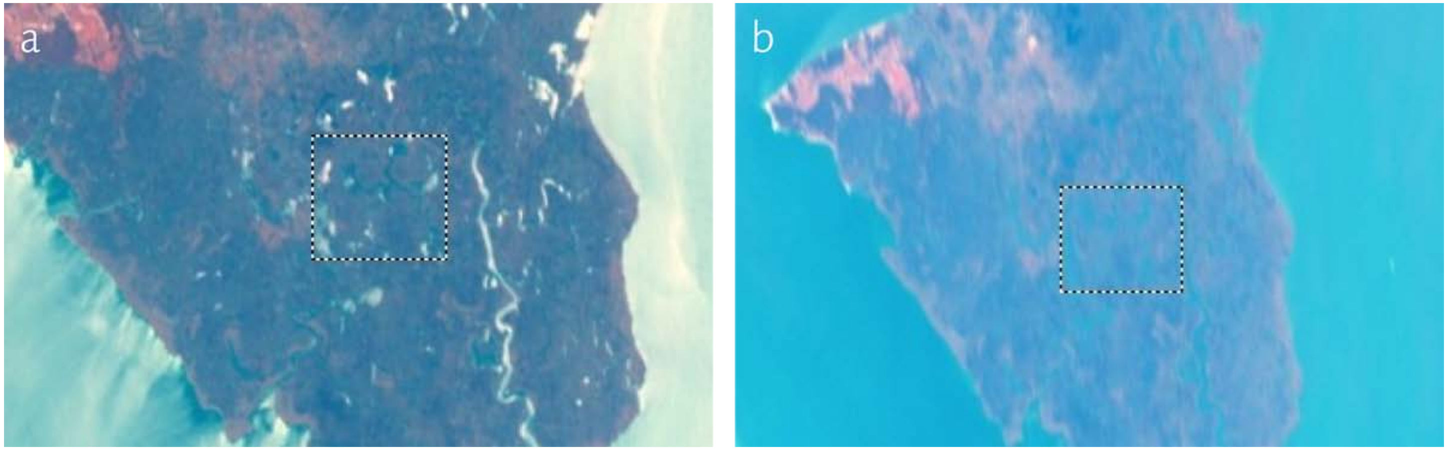

Spectra extracted from regions highlighted by boxes above. (a) At 0° nominal view zenith angle, glint produces very high values across the spectrum, evidenced by the maximum spectral curve. (b) At 55° nominal view zenith angle, the glint effect is greatly reduced.

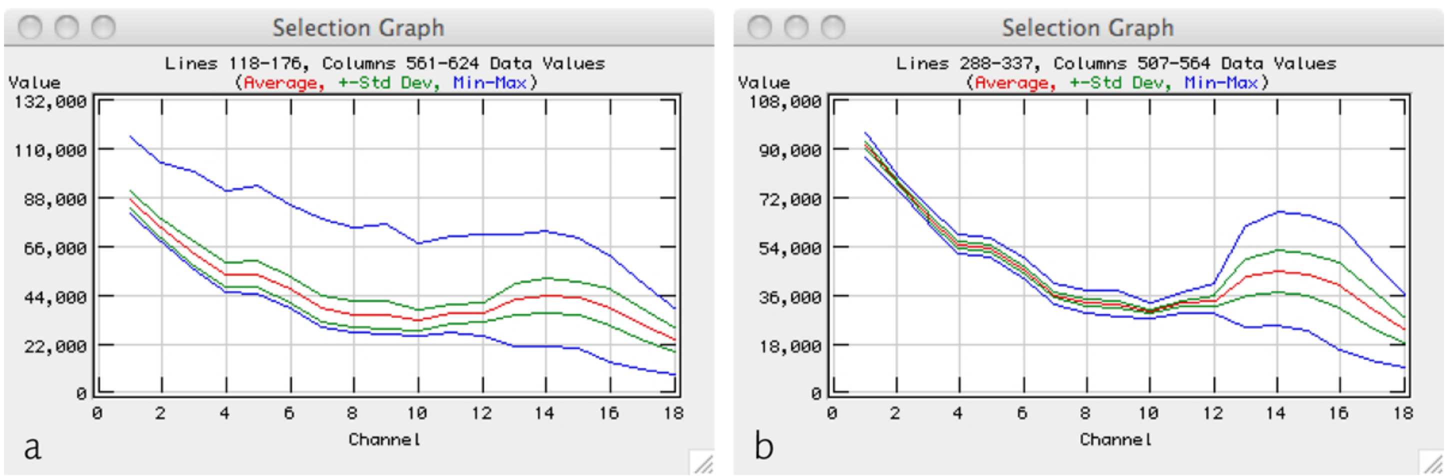

Source: Kevin Turpie

Glint Impact on HyspIRI Science: Summary

- For two basic HyspIRI science objectives, coral reefs and seagrass, expected levels of glint do not appear to dramatically impact classification retrievals.
- Glint has the greatest impact when retrieval conditions are already marginal, for example when water column optical properties limit penetration depth.
- Potential for improvement via mitigation for glint was not investigated.

- For the open ocean, with very low suspended chlorophyll levels, it is clear that glint correction must be tied to correction for atmospheric aerosols.
- Thus, both are fundamental requirements for accurate retrieval of spectral remote sensing reflectance.

- The situation is less clear for glint effects in emergent vegetation.
- Measurement and modeling capabilities for these systems lag those for shallow and deep oceans.
- At the same time, emergent vegetation has the benefit of usefully observable NIR and SWIR spectral features.

Mitigation Options
Avoidance

- Avoidance is the simplest method for mitigation of glint impacts, and it is the method of choice in operational ocean color.
- Any portions of imagery that exhibit significant glint can merely be ignored, then re-imaged on subsequent satellite overpasses.
- Nearshore and benthic applications typically require higher spatial resolution, i.e., 1–100 m vs. 1 km.
- The higher spatial resolution required closer to shore is offset by narrower fields of view and longer revisit times.
- The data rate for a given area of Earth surface is much lower, and it is generally not possible to ignore image data that exhibit glint effects.
- Thus, glint avoidance is a luxury not often afforded to nearshore and benthic applications.

Mitigation Options

NIR-VIS Empirical Linear Relationships

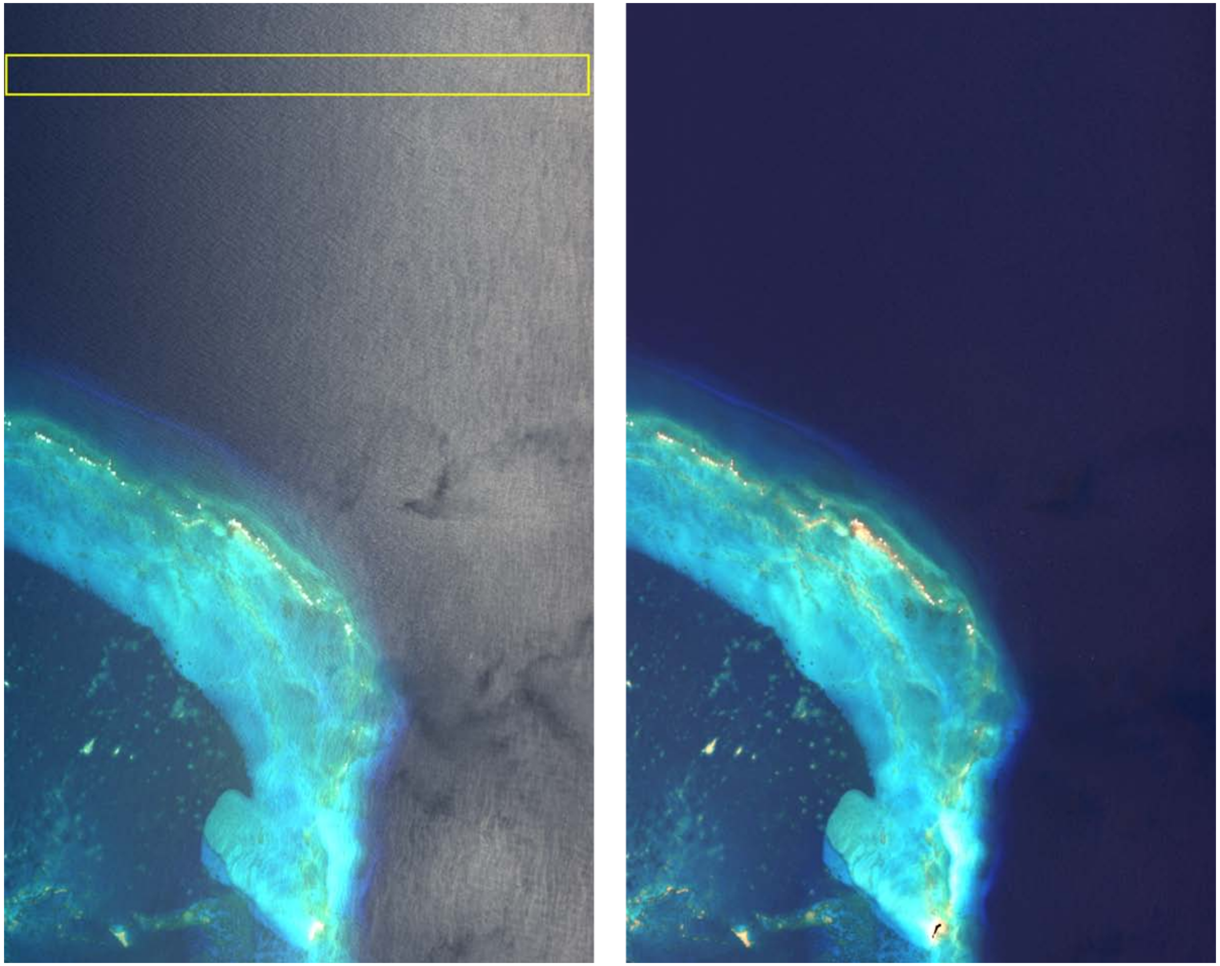

AVIRIS scene f000418t01p03_r01 covering the southeast portion of French Frigate Shoals, Hawaii and surrounding deep ocean. Image is rotated so that north is to the left of the scene. (Left) Original scene shows very strong glint effects. Yellow box highlights region from which empirical linear relationships are derived. (Right) The scene after application of glint correction. Glint effects are very effectively removed.

Mitigation Options

Subtraction of NIR Reflectance

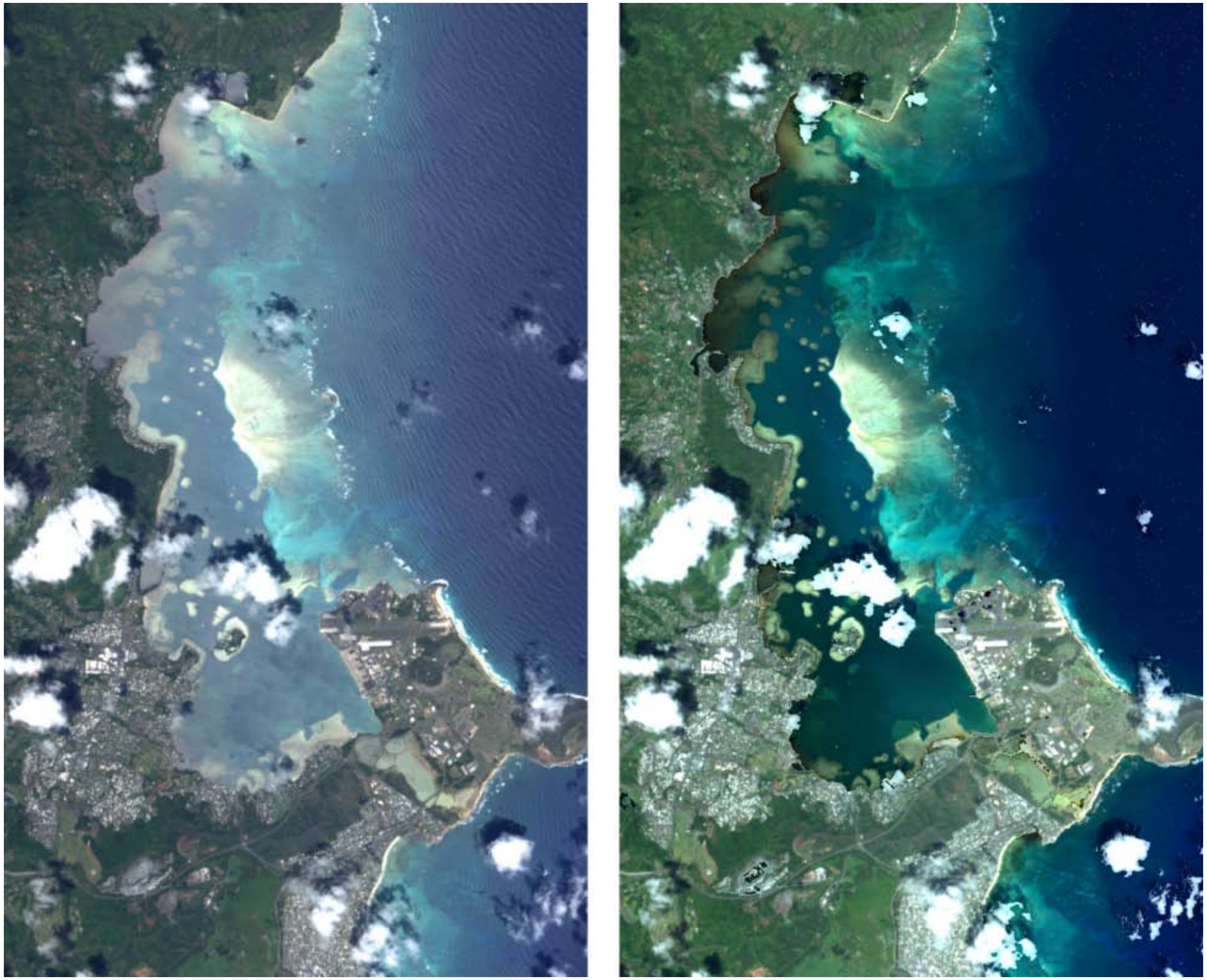

Example of glint correction using subtraction of NIR reflectance. (Left) Original AVIRIS scene of Kaneohe Bay, Hawaii (f000412t01p03_r08). (Right) The scene after atmosphere and glint correction. Clouds and some sea surface features remain; this is due to automated masking. Overall, glint correction performs quite well.

Source: Bo-Cai Gao

Mitigation Options

Uniform Spectral Offset

$$R_{rs}(\lambda) = R_{rs}^{*}(\lambda) - R_{rs}(750) + \Delta,$$

where

$$\Delta = 0.00019 + 0.1[R_{rs}^{*}(640) - R_{rs}^{*}(750)]$$

Source: James Goodman

Glint-Aerosol Discrimination

At-sensor reflectance

$$\rho_t = \rho_r + \rho_a + \rho_{sky}^{TOA} + \rho_g^{TOA} + \frac{\rho_w^{SFC} \cdot T_{gas} \cdot t_d \cdot t_u}{1 - s \cdot \rho_w^{SFC}}$$

For $\lambda > 1000$ nm, this reduces to

$$\rho_t - \rho_r - \rho_{sky}^{TOA} = \rho_a + \rho_g^{TOA}$$

Spectral decomposition relies on glint and aerosol spectral shapes

$$\rho_a(\lambda) = \rho_{a0} \cdot A(\lambda) \qquad \text{and} \qquad \rho_g^{TOA}(\lambda) = \rho_{g0} \cdot A(\lambda)$$

$A(\lambda)$ and $G(\lambda)$ are obtained using raditive transfer simulations.

Solve for ρ_{a0} and ρ_{g0}, then extrapolate to VIS.

Source: Youngje Park

Conclusions and Recommendations

Conclusions

- The literature and present examples demonstrate that glint correction is feasible.
- Present examples further demonstrate that key HyspIRI science objectives are achievable even in the presence of glint.
- Therefore, it is very reasonable that active glint correction can be a part of a successful HyspIRI processing flow.

Near-Term Recommendations

- The glint correction procedures described here each demonstrate strong potential. Each also requires further refinement.
- The presented analyses have touched on some key points about glint and its impact on remote sensing retrievals of certain biophysical parameters. These issues could certainly benefit from deeper investigation.
- It would be very desirable to perform field validation for model results of selected, important HyspIRI science objectives.

Long-Term Recommendations

- Environmental optics would be greatly advanced by the collection of a few comprehensive data sets that provide all inputs and outputs to the RTE.
- As glint correction procedures become codified, it would be useful to have a glint toolbox utility from which a user could select among a suite of glint correction techniques.